

Five heterometallic Sr^{II}–M^{II} (M = Co, Ni, Zn, Cu) 3-D coordination polymers: Synthesis, structures and magnetic properties



Yanmei Chen^{a,b}, Qian Gao^a, Haifeng Zhang^a, Dandan Gao^b, Yahong Li^{a,c,*}, Wei Liu^a, Wu Li^b

^a Key Laboratory of Organic Synthesis of Jiangsu Province, College of Chemistry, Chemical Engineering and Materials Science, Soochow University, Suzhou 215123, China

^b Key Laboratory of Salt Lake Resources and Chemistry, Qinghai Institute of Salt Lakes, Chinese Academy of Sciences, Xining 810008, China

^c State Key Laboratory of Applied Organic Chemistry, Lanzhou University, Lanzhou 730000, China

ARTICLE INFO

Article history:

Received 7 November 2013

Accepted 28 December 2013

Available online 11 January 2014

Keywords:

Pyridine-2,3-dicarboxylic acid

Heterometallic complexes

Alkaline earth metal

Magnetic properties

ABSTRACT

Five heterometallic coordination polymers based on pyridine 2,3-dicarboxylic acid (H₂pydc), namely [MSr(pydc)₂(H₂O)₂]_n (M = Co (**1**), Ni (**2**)), [MSr₂(pydc)₃(H₂O)₄]_n·2nH₂O (M = Ni (**3**), Zn (**4**)) and [CuSr(pydc)₂(H₂O)₃]_n·2nH₂O (**5**), have been synthesized via rationally choosing the appropriate metal salts and dexterously adjusting the pH values of the reaction system. X-ray crystallographic analyses reveal that the polymers display three varieties of 3-D framework structures. The magnetic properties of complexes **1** and **2** were investigated, and antiferromagnetic M^{II}...M^{II} interactions were found for both complexes.

© 2014 Elsevier Ltd. All rights reserved.

1. Introduction

Heterometallic coordination polymers containing both transition metals and alkaline earth metals are currently being widely investigated due to the pleasing architectures that many such complexes possess and their potential applications in the fields of catalysis, material science and biochemistry [1–5]. However, the involvement of alkaline earth metals in heterometallic complexes is challengeable, and chemists are often frustrated by obtaining homometallic coordination polymers instead of heterometallic ones. The most important reasons are as follows [6]: (i) the transition metal ions have a strong tendency to coordinate both nitrogen and oxygen atoms, whereas the alkaline earth metals prefer oxygen donors to nitrogen donors. They will compete for oxygen atoms; (ii) the broad span of coordination numbers of alkaline earth metals makes the topologies of the coordination polymers uncontrollable. Hence, it is of high demand to discover an efficient approach to incorporate both transition metals and alkaline earth metals into one coordination system. Recent advances have revealed that N-heterocyclic carboxylates are useful to combine alkaline earth metals with transition metals [7–9]. Alkaline earth metals are firstly coordinated by the oxygen atoms to form “complex-ligands”, then the “complex-ligands” bind with transition metal ions to generate heterometallic coordination polymers [5,9–19].

In our previous work, we have reported two series of heterometallic coordination polymers, Sr^{II}–Cu^{II} [6] and Sr^{II}–Ln^{III} [20,21], based on N-heterocyclic carboxylate ligands. They were all constructed by employing ‘complex-ligands’ of Sr^{II} ions. As a continuation of our previous studies, we have investigated the synthetic chemistry of heterometallic Sr^{II}–M^{II} (M = Co, Ni, Zn, Cu) coordination polymers by employing pyridine 2,3-dicarboxylic acid (H₂pydc) as a ligand. Pyridine 2,3-dicarboxylic acid can coordinate with either transition metals or alkaline earth metals to form coordination complexes [22–33]. However, other than two heterometallic complexes (Co–Ca, Co–Ba) reported by the Lazarescu group [22], no heterometallic complexes containing both strontium and transition metals and supported by pyridine 2,3-dicarboxylic acid have been reported.

Herein, we present the synthesis and characterization of the first series of M^{II}–Sr^{II} heterometallic complexes, [MSr(pydc)₂(H₂O)₂]_n (M = Co (**1**), Ni (**2**)), [MSr₂(pydc)₃(H₂O)₄]_n·2nH₂O (M = Ni (**3**), Zn (**4**)) and [CuSr(pydc)₂(H₂O)₃]_n·2nH₂O (**5**), based on pyridine-2,3-dicarboxylic acid. These complexes display three varieties of 3-D framework structures. The magnetic properties of complexes **1** and **2** were also investigated.

2. Experimental

2.1. General procedures

All manipulations were performed under aerobic and solvothermal conditions. The reagents and solvents were purchased from commercial suppliers and used without further purification. The

* Corresponding author at: Key Laboratory of Organic Synthesis of Jiangsu Province, College of Chemistry, Chemical Engineering and Materials Science, Soochow University, Suzhou 215123, China.

E-mail address: liyahong@suda.edu.cn (Y. Li).

C, H and N microanalyses were carried out with a Carlo-Erba EA1110 CHNO-S elemental analyzer. FT-IR spectra were recorded from KBr pellets in the range 400–4000 cm^{-1} on a Nicolet Magna-IR 500 spectrometer. Powder X-ray diffraction (PXRD) data were recorded on a Rigaku D/Max-2500 diffractometer at 40 kV and 100 mA with a Cu-target tube and a graphite monochromator. Thermal gravimetric analysis (TGA) was conducted on a NETZSCH STA 449F3 instrument in flowing N_2 with a heating rate of 5 $^\circ\text{C}/\text{min}$. Magnetic susceptibility measurements were performed in the temperature range 2–300 K, using a Quantum Design MPMS XL-7 SQUID magnetometer.

2.2. Crystal structure refinement

Data were collected at room temperature on a Bruker Smart ApexII diffractometer equipped with a graphite monochromator utilizing Mo $\text{K}\alpha$ radiation ($\lambda = 0.71073 \text{ \AA}$); the ω and φ scan technique was applied. The structures were solved by direct methods using SHELXS-97 [34] and refined on F^2 using full-matrix least-squares with SHELXL-97 [35,36]. Hydrogen atoms of water molecules were localized from a difference Fourier map and the positions of the remaining H atoms were located in geometrically calculated positions. It should be noted that the hydrogen atoms of the water molecules (O13) in **3** and **4** were not located and thus some B-type errors related to the CIF-check files may be observed. Crystallographic data together with refinement details for **1–5** are summarized in Table 1. See CIF files for further details.

2.3. Preparations

2.3.1. Synthesis of $[\text{MSr}(\text{pydc})_2(\text{H}_2\text{O})_2]_n$ ($M = \text{Co}$ (**1**), Ni (**2**))

A mixture of H_2pydc (0.0333 g, 0.2 mmol), $\text{Sr}(\text{OH})_2 \cdot 8\text{H}_2\text{O}$ (0.0266 g, 0.1 mmol), $\text{Co}(\text{CH}_3\text{COO})_2 \cdot 4\text{H}_2\text{O}$ (0.0247 g, 0.1 mmol) [or $\text{Ni}(\text{CH}_3\text{COO})_2 \cdot 4\text{H}_2\text{O}$ (0.0256 g, 0.1 mmol)], $\text{H}_2\text{O}/\text{C}_2\text{H}_5\text{OH}$ (2 mL, $v/v = 2:1$) was sealed in a 6 mL Pyrex-tube. The tube was heated at 120 $^\circ\text{C}$ for 1 day under autogenous pressure. Cooling of the

resultant solution to room temperature gave crystals of the product. The yields of **1** and **2** are 0.0330 g (65%, based on Co) and 0.0283 g (55%, based on Ni), respectively. *Anal. Calc.* for $\text{CoSrC}_{14}\text{H}_{10}\text{N}_2\text{O}_{10}$ (**1**, orange rod crystals): C, 32.86; H, 1.77; N, 5.47. Found: C, 32.65; H, 1.99; N, 5.45%. Selected IR data (KBr, cm^{-1}): 3472(w), 3078(s), 1613(s), 1573(s), 1462(s), 1413(s), 1385(s), 1108(s), 850(s), 779(s), 733(s), 711(s), 672(s). *Anal. Calc.* for $\text{NiSrC}_{14}\text{H}_{10}\text{N}_2\text{O}_{10}$ (**2**, light-blue acicular crystals): C, 32.81; H, 1.97; N, 5.47. Found: C, 32.62; H, 2.29; N, 5.46%. Selected IR data (KBr, cm^{-1}): 3474(w), 3081(s), 1615(s), 1574(s), 1456(s), 1413(s), 1387(s), 1111(s), 852(s), 840(s), 736(s), 711(s), 677(s).

2.3.2. Synthesis of $[\text{MSr}_2(\text{pydc})_3(\text{H}_2\text{O})_4]_n \cdot 2n\text{H}_2\text{O}$ ($M = \text{Ni}$ (**3**), $M = \text{Zn}$ (**4**))

A mixture of H_2pydc (0.0333 g, 0.2 mmol), $\text{SrCl}_2 \cdot 6\text{H}_2\text{O}$ (0.0266 g, 0.1 mmol), $\text{Ni}(\text{CH}_3\text{COO})_2 \cdot 4\text{H}_2\text{O}$ (0.0251 g, 0.1 mmol) [or $\text{Zn}(\text{CH}_3\text{COO})_2 \cdot 2\text{H}_2\text{O}$ (0.0219 g, 0.1 mmol)], imidazole (0.0319 g, 0.469 mmol) and $\text{H}_2\text{O}/\text{C}_2\text{H}_5\text{OH}$ (2 mL, $v/v = 2:1$) was sealed in a 6 mL Pyrex-tube and heated at 120 $^\circ\text{C}$ for 1 day under autogenous pressure. Cooling of the mixture to room temperature gave crystals of the product. The yields of **3** and **4** are 0.0235 g (56%, based on Sr) and 0.0254 g (60%, based on Sr), respectively. *Anal. Calc.* for $\text{NiSr}_2\text{C}_{21}\text{H}_{21}\text{N}_3\text{O}_{18}$ (**3**, blue platy crystals): C, 30.12; H, 2.53; N, 5.02. Found: C, 29.67; H, 2.74; N, 5.08%. Selected IR data (KBr, cm^{-1}): 3448(w), 1613(s), 1569(s), 1400(s), 1112(s), 843(s), 7101(s), 675(s). *Anal. Calc.* for $\text{ZnSr}_2\text{C}_{21}\text{H}_{21}\text{N}_3\text{O}_{18}$ (**4**, colorless platy crystals): C, 29.88; H, 2.51; N, 4.98. Found: C, 29.51; H, 2.72; N, 4.81%. Selected IR data (KBr, cm^{-1}): 3453(w), 1614(s), 1572(s), 1446(s), 1382(s), 1275(s), 1238(s), 1113(s), 881(s), 843(s), 787(s), 710(s).

2.3.3. Synthesis of $[\text{CuSr}(\text{pydc})_2(\text{H}_2\text{O})_3]_n \cdot 2n\text{H}_2\text{O}$ (**5**)

Complex **5** was prepared by the same procedure as that of **3**, using $\text{CuCl}_2 \cdot 2\text{H}_2\text{O}$ (0.0171 g, 0.1 mmol) instead of $\text{Ni}(\text{CH}_3\text{COO})_2 \cdot 4\text{H}_2\text{O}$ as the starting material. Blue bar crystals of **5** were obtained. The crystals were collected by filtration, washed with H_2O (3 mL)

Table 1
Crystallographic data and structure refinement for complexes **1–5**.

	1	2	3	4	5
Formula ^a	$\text{CoSrC}_{14}\text{H}_{10}\text{N}_2\text{O}_{10}$	$\text{NiSrC}_{14}\text{H}_{10}\text{N}_2\text{O}_{10}$	$\text{NiSr}_2\text{C}_{21}\text{H}_{21}\text{N}_3\text{O}_{18}$	$\text{ZnSr}_2\text{C}_{21}\text{H}_{21}\text{N}_3\text{O}_{18}$	$\text{SrCuC}_{14}\text{H}_{16}\text{N}_2\text{O}_{13}$
M (g mol^{-1}) ^a	512.79	512.57	837.36	844.02	571.46
T (K)	569(2)	569(2)	569(2)	569(2)	569(2)
λ (\AA) ^b	0.71073	0.71073	0.71073	0.71073	0.71073
Crystal system	orthorhombic	orthorhombic	triclinic	triclinic	triclinic
Space group	$Pnma$	$Pnma$	$P\bar{1}$	$P\bar{1}$	$P\bar{1}$
a (\AA)	7.891(3)	7.8101(13)	7.834(5)	7.875(7)	6.593(4)
b (\AA)	16.554(7)	16.489(3)	13.782(9)	13.898(13)	10.723(7)
c (\AA)	12.826(5)	12.635(2)	13.798(9)	13.910(13)	14.033(9)
α ($^\circ$)	90.00	90.00	107.577(10)	107.624(12)	94.269(12)
β ($^\circ$)	90.00	90.00	97.328(10)	97.416(14)	101.964(12)
γ ($^\circ$)	90.00	90.00	97.034(10)	97.310(13)	92.428(11)
Volume (\AA^3)	1675.5(12)	1627.2(5)	1388.0(16)	1416(2)	966.1(11)
Z	4	4	2	2	2
ρ (mg mm^{-3})	2.033	2.092	2.004	1.979	1.964
μ (mm^{-1})	4.236	4.499	4.592	4.682	3.936
$F(000)$	1012	1016	832	836	570
2θ range ($^\circ$)	4.02–54	4.06–49.98	3.66–49.98	5.08–50	5.04–48.48
Measured/independent	9910/1892	8319/1488	16017/4881	15530/4973	4832/3032
R_{int} reflections	0.0387	0.0409	0.0368	0.0377	0.0382
R_1^c	0.0279	0.0335	0.0921	0.1068	0.0980
$wR_2^{d,e}$	0.0916	0.0932	0.2473	0.2769	0.3049
GOF on F^2	1.069	1.063	1.033	1.077	1.099

^a Including solvate molecules.

^b Mo $\text{K}\alpha$ radiation.

^c $R_1 = \sum(|F_o| - |F_c|) / \sum(|F_o|)$ for observed reflections.

^d $w = 1/[\sigma^2(F_o^2) + (aP)^2 + bP]$ and $P = [\max(F_o^2, 0) + 2F_c^2]/3$.

^e $wR_2 = \sum[w(F_o^2 - F_c^2)^2] / \sum[w(F_o^2)^2]^{1/2}$ for all data.

and dried in air. Yield: 0.0198 g (35%, based on Cu). *Anal. Calc.* for $C_{14}H_{12}CuN_2O_{11}Sr$: C, 29.43; H, 2.82; N, 4.90. Found: C, 29.61; H, 2.72; N, 4.96%. Selected IR data (KBr, cm^{-1}): 3439(m), 1619(s), 1586(s), 1377(s), 1118(s), 881(s), 837(s), 728(s), 704(s), 475(s).

3. Results and discussion

3.1. Synthesis

It is known that numerous factors, including the pH values of the systems, metal sources and solvents, influence the formation of the heterometallic coordination polymers. $Sr(OH)_2 \cdot 8H_2O$ is a better metal source than $SrCl_2 \cdot 6H_2O$ in the preparation of **1**. It is believed that $Sr(OH)_2 \cdot 8H_2O$ is used not only as the metal source but also as an alkaline to adjust the pH value of the reaction system of **1**.

For the preparation of **4** and **5**, we found that imidazole is a better base than $Sr(OH)_2 \cdot 8H_2O$ for adjusting the pH value of the systems. The yields of **4** and **5** using $SrCl_2 \cdot 6H_2O$ and imidazole as the metal source and alkaline, respectively, are much higher than those employing $Sr(OH)_2 \cdot 8H_2O$ as the metal source. However, it is interesting to note that two distinct complexes, **2** and **3**, were generated on employing $Sr(OH)_2 \cdot 8H_2O$ or $SrCl_2 \cdot 6H_2O$ and imidazole as the reagents. This strategy for the rational assembly of heterometallic coordination polymers via dexterously choosing the appropriate reagents as metal sources as well as alkaline has rarely been reported [6], reflecting the synthetic novelty of this work.

It is intriguing that no crystals were obtained when copper acetate was used as the starting material. However, the reaction of H_2pydc , $SrCl_2 \cdot 6H_2O$, imidazole and $CuCl_2 \cdot 2H_2O$ led to the isolation of **5** as blue crystals.

EtOH plays a vital role in the crystal growth process. In the absence of EtOH, powder forms of the coordination polymers were obtained. EtOH may hinder the diffusion of crystallization nutrients in the reaction system and make the crystal growth slower and more homogeneous [37].

The methods for the synthesis of **1–5** were summarized in Scheme 1.

3.2. Description of structures

3.2.1. Structure of $[MSr(pydc)_2(H_2O)_2]_n$ ($M = Co$ (**1**), $M = Ni$ (**2**))

The crystal structure determination reveals that complexes **1** and **2** are isostructural. The structure of **1** will be discussed here in detail. Complex **1** exhibits a 3-D framework structure (Fig. 1). The Co^{II} ion is six-coordinated by four oxygen atoms (O1, O1E, O4C, O4F) and two nitrogen atoms (N1, N1E) of four $pydc^{2-}$ anions (Fig. 1a). Each Co^{II} ion is connected to eight Sr^{II} ions by four carboxylic groups (O1–C6–O2, O1E–C6E–O2E, O4C–C7C–O3C, O4F–C7F–O3F) of four $pydc^{2-}$ ligands (in coordination mode A of Scheme 2). The Sr^{II} ion is eight-coordinated by six carboxylate oxygen atoms (O2, O2A, O2B, O2C, O3, O3A) of four $pydc^{2-}$ ligands and two terminal water molecules (O5, O6) in a slightly distorted dodecahedral geometry (Fig. 1b). Each Sr^{II} ion is connected to two

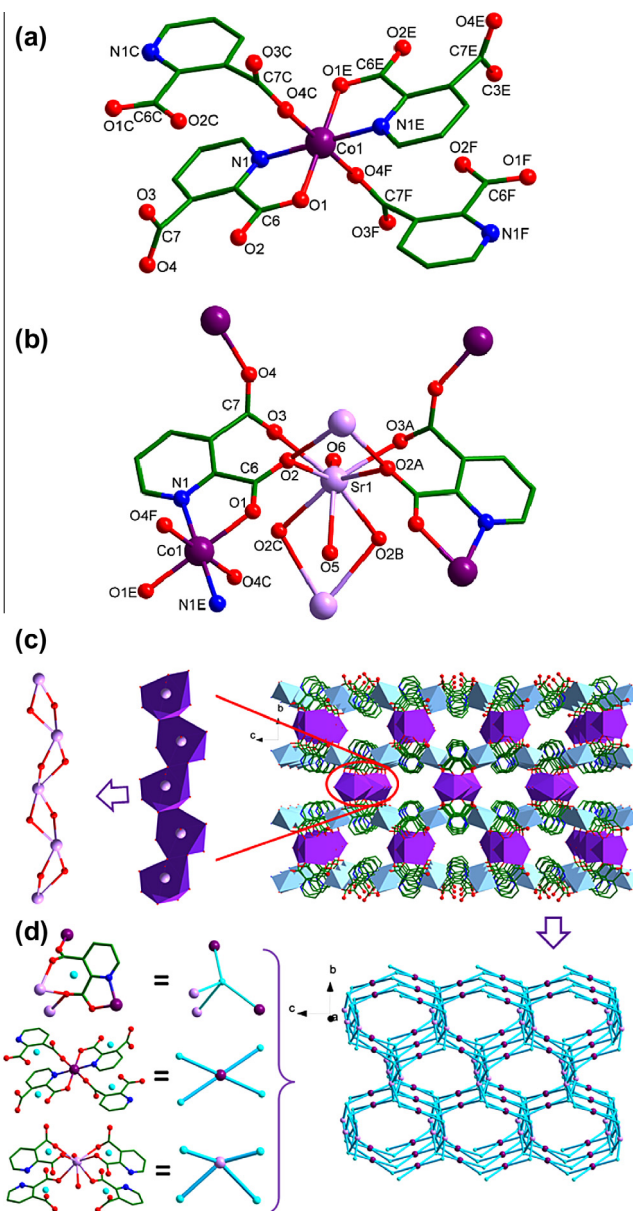
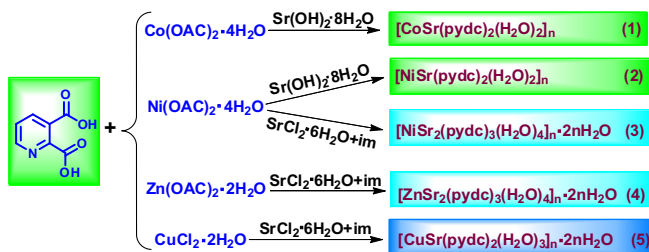


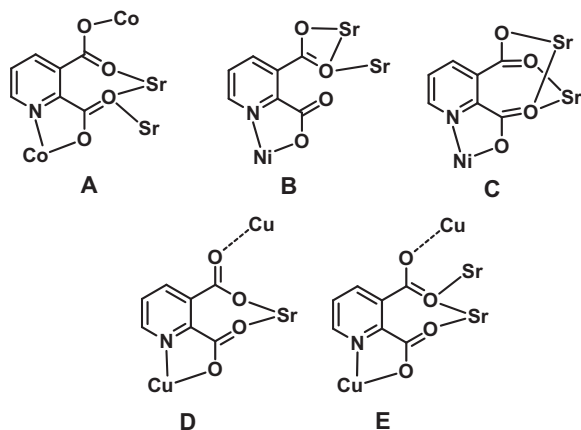
Fig. 1. (a) Coordination environments of the Co^{II} ions in **1**. (b) Coordination environments of the Sr^{II} ions in **1** (A: $x, -y + 3/2, z$; B: $x + 1/2, -y + 3/2, -z + 3/2$; C: $x + 1/2, y, -z + 3/2$; D: $x - 1/2, y, -z + 3/2$; E: $-x + 1, -y + 1, -z + 2$; F: $-x + 1/2, -y + 1, z + 1/2$). (c) The polyhedron structure of the 3-D framework of **1** viewed along the a -axis and schematic representation of the 3-nodal topology net with the topological notation $(4^2.8^2.10^2)(4^3.6^2.8)_2(4^4.6^2)$ in the bc plane. Hydrogen atoms are omitted for clarity. Color codes: lavender, Sr; violet, Co; red, O; blue, N; green, C. (Colour online.)

neighboring Sr^{II} ions by two μ_2 -O atoms to form a 1-D $[Sr(O)_2Sr]_n$ chain structure viewed along the a -axis (Fig. 1c). The 1-D $[Sr(pydc)_2]_n^{2n-}$ chains are connected by Co^{II} ions through $pydc^{2-}$ ligands to form a 3-D framework structure (Fig. 1c). The intramolecular hydrogen bonds between coordinated water molecules as the hydrogen donors and carboxylate oxygen atoms as hydrogen acceptors enhance the stability of the framework structure (Fig. S1).

The $pydc^{2-}$ ligand acts as a μ_4 -bridge, linking two Co^{II} ions and two Sr^{II} ions. To better understand the 3-D framework structure, a topological approach has been applied. The $pydc^{2-}$ ligand can be simplified to a 4-connected node, as shown in Fig. 1c, and the Co^{II} and Sr^{II} ions can also be simplified to a 4-connected node. The



Scheme 1. Synthesis of complexes **1–5**.



Scheme 2. Coordination modes of the pydc^{2-} anions in **1–5** (dotted line represents the longer bond lengths originated from the Jahn–Teller effect).

overall structure of **1** can be simplified to a new 3-nodal 4,4,4-c net with a Schläfli symbol of $(4^2.8^2.10^2)(4^3.6^2.8)_2(4^4.6^2)$ [38,39].

3.2.2. Structure of $[\text{MSr}_2(\text{pydc})_3(\text{H}_2\text{O})_4]_n \cdot 2n\text{H}_2\text{O}$ ($M = \text{Ni}$ (**3**), $M = \text{Zn}$ (**4**))

X-ray crystallography analyses reveal that complexes **3** and **4** are isostructural. Complex **3** is taken here as a representative example to depict the structure in detail. The asymmetric unit of **3** consists of one Ni^{II} ion, three pydc^{2-} anions, two Sr^{II} ions, four coordinated water molecules and two lattice water molecules. As shown in Fig. 2a, the Ni1 center is six-coordinated by three oxygen atoms (O1, O5D, O9) and three nitrogen atoms (N1, N2D, N3) from three pydc^{2-} anions (two are in coordination mode B and one is in coordination mode C) to form a $[\text{Ni}(\text{pydc})_3]^{4-}$ unit. Each $[\text{Ni}(\text{pydc})_3]^{4-}$ moiety is connected to six Sr^{II} ions through the carboxylic groups of the pydc^{2-} ligands.

The coordination numbers of Sr1 and Sr2 ions are seven and nine, respectively. The Sr1 ion (Fig. 2b) is coordinated by four carboxylate oxygen atoms (μ_2 -O7B, μ_2 -O8, μ_2 -O11A, μ_2 -O4) from four pydc^{2-} ligands and three terminal water molecules (O13, O14, O16). The Sr2 ion (Fig. 2c) is coordinated by eight oxygen atoms (O3, μ_2 -O4, μ_2 -O6, μ_2 -O8, μ_2 -O11A, O12A, μ_2 -O6E, μ_2 -O7E) of four pydc^{2-} ligands and one terminal water molecule (O15).

The Ni1F and Ni1K ions are connected to Sr2 ions through carboxylic groups O6–C13–O5 and O6E–C13E–O5E, respectively (Fig. 2d). The Sr1 ions and Sr2 ions are bridged by μ_2 -O atoms or carboxylic groups to form a 1-D chain structure along the *a*-axis. The chains are bridged by $[\text{Ni}(\text{pydc})_3]^{4-}$ units to form a 3-D framework structure (Fig. 2e). Moreover, intramolecular hydrogen bonds between coordination water molecules as hydrogen donors and carboxylate oxygen atoms as hydrogen acceptors are observed (Fig. S2).

The pydc^{2-} ligands display coordination modes B and C in Scheme 2. All of the pydc^{2-} ligands act as a μ_3 -bridge, linking one Ni^{II} ion and two Sr^{II} ions. A topological approach has been applied to simplify the nature of the 3-D framework. Each Ni^{II} ion can be considered as a 3-connected node, every four neighboring Sr^{II} ions (two Sr1 and two Sr2 ions) can be considered as an 8-connected node and each pydc^{2-} ligand, serving as a linear linker, connects adjacent 3-connected and 8-connected nodes (Fig. 3f). The whole structure can be simplified to a 2-nodal 3,8-c topology net with a Schläfli symbol of $(4^3)_2(4^6.6^{18}.8^4)$ [39]. The topological type is tfz-d.

3.2.3. Structure of $[\text{CuSr}(\text{pydc})_2(\text{H}_2\text{O})_3]_n \cdot 2n\text{H}_2\text{O}$ (**5**)

X-ray single-crystal diffraction analysis reveals that complex **5** exhibits a 3-D network structure. As shown in Fig. 3a, the Sr1 ion

is eight-coordinated by five carboxylate oxygen atoms (O2, O3, O6, O7, O7A) of three pydc^{2-} ligands and three terminal water molecules (O9, O10, O11) in a slightly distorted dodecahedral geometry. Two Sr^{II} ions are bridged by two carboxylate oxygen atoms (μ_2 -O7, μ_2 -O7A) to form a $[\text{Sr}_2(\text{pydc})_4]^{4-}$ unit. Each Sr^{II} ion is connected to one Cu1 ion by the carboxylic group O2–C6–O1, and linked to two Cu2 ions by the carboxylate groups O6–C13–O5 and O7–C14–O8.

The Cu1 ion is six-coordinated by four carboxylate oxygen atoms (O1, O1F, O4E, O4G) and two nitrogen atoms (N1, N1F) of four pydc^{2-} ligands in a distorted octahedral geometry (Fig. 3b). The Cu1–O1 and Cu1–N1 distances are 1.954(10) and 1.969(12) Å, respectively. The Cu1–O4E and Cu1–O4G distances are 2.529(11) Å, and this bond length difference may be caused by the Jahn–Teller effect [40,41]. Each Cu1 ion is connected to four Sr^{II} ions and other two Cu1 ions by four pydc^{2-} ligands (in coordination mode D).

The Cu2 ion is six-coordinated (Fig. 3c). It is chelated by two pydc^{2-} ligands with four atoms (N2, O5, N2B, O5B), and is coordinated by two oxygen atoms (O8C, O8D), showing the Jahn–Teller effect [40,41]. The Cu2–N2, Cu2–O5 and Cu2–O8C distances are 1.967(11), 1.962(11) and 2.485(9) Å, respectively. Each Cu2 ion is connected to eight Sr^{II} ions and two Cu2 ions through the pydc^{2-} ligands (in coordination mode E). The $[\text{Sr}_2(\text{pydc})_4]^{4-}$ units are connected by Cu1 ions to form a 2-D network in the *ac* plane (Fig. 3d). The 2-D networks are connected by Cu2 ions to form a 3-D framework structure (Fig. 3e). In addition, hydrogen bonds between lattice water molecules (or coordination water molecules) as hydrogen donors and carboxylate oxygen atoms of pydc^{2-} ligands as acceptors are observed (Fig. S3).

The pydc^{2-} ligands display two kinds of coordination modes (D and E). To better understand the 3-D network of the structure, a topological approach has been applied. As shown in Fig. 3f, each two neighboring Sr^{II} ions can be simplified to a 4-connected node with the point symbol 8^6 . Each pydc^{2-} ligand can be simplified to a 3-connected node with point symbol 4.8^2 , and each Cu^{II} ion can be simplified to a 4-connected node with point symbol $4^2.8^2.10^2$. The nature of the 3-D framework structure of **5** can be simplified to a 3-nodal 3,4,4-c net with a Schläfli symbol of $(4.8^2)_4(4^2.8^2.10^2)_2(8^6)$ [39]. The topological type is sqc945.

Complexes **1–5** join a very small family of $\text{M}^{\text{II}}\text{–AE}^{\text{II}}$ ($M = \text{Co}$; $\text{AE} = \text{Ca}$ and Ba) [22] coordination polymers supported by pyridine 2,3-dicarboxylic acid, whereas the structures of **1–5** are totally different from those of the reported complexes. Complexes **1–5** all exhibit 3-D framework structures, however, the topological architectures are totally different, revealing the structure diversity of the $\text{M}^{\text{II}}\text{–AE}^{\text{II}}$ coordination polymers.

3.3. XRD patterns and thermal properties

In order to check the phase purity of the complexes, the powder X-ray diffractions (PXRD) of **1–5** have been measured and compared with those simulated from the single-crystal structures. The measured PXRD patterns of **1–5** are in good agreement with the patterns generated from their single crystal data (Fig. S9), indicating the phase purity of the samples. The differences in intensity are due to the preferred orientation of the powder samples.

The thermogravimetric analyses were performed under an N_2 atmosphere in the temperature range 30–1250 °C. The results reveal that complexes **1–5** possess two obvious steps of weight loss (Fig. 4). The first weight loss occurs in the range 30–220 °C, with a weight loss of 7.36%, 8.61%, 14.17%, 13.86% and 15.99%, respectively, which corresponds to the loss of all coordinated and lattice water molecules (Calc. 7.03%, 7.02%, 12.90%, 12.80% and 15.75%, respectively). Above 300 °C, the frameworks begin to collapse and these compounds are gradually decomposed to complicated oxides. The

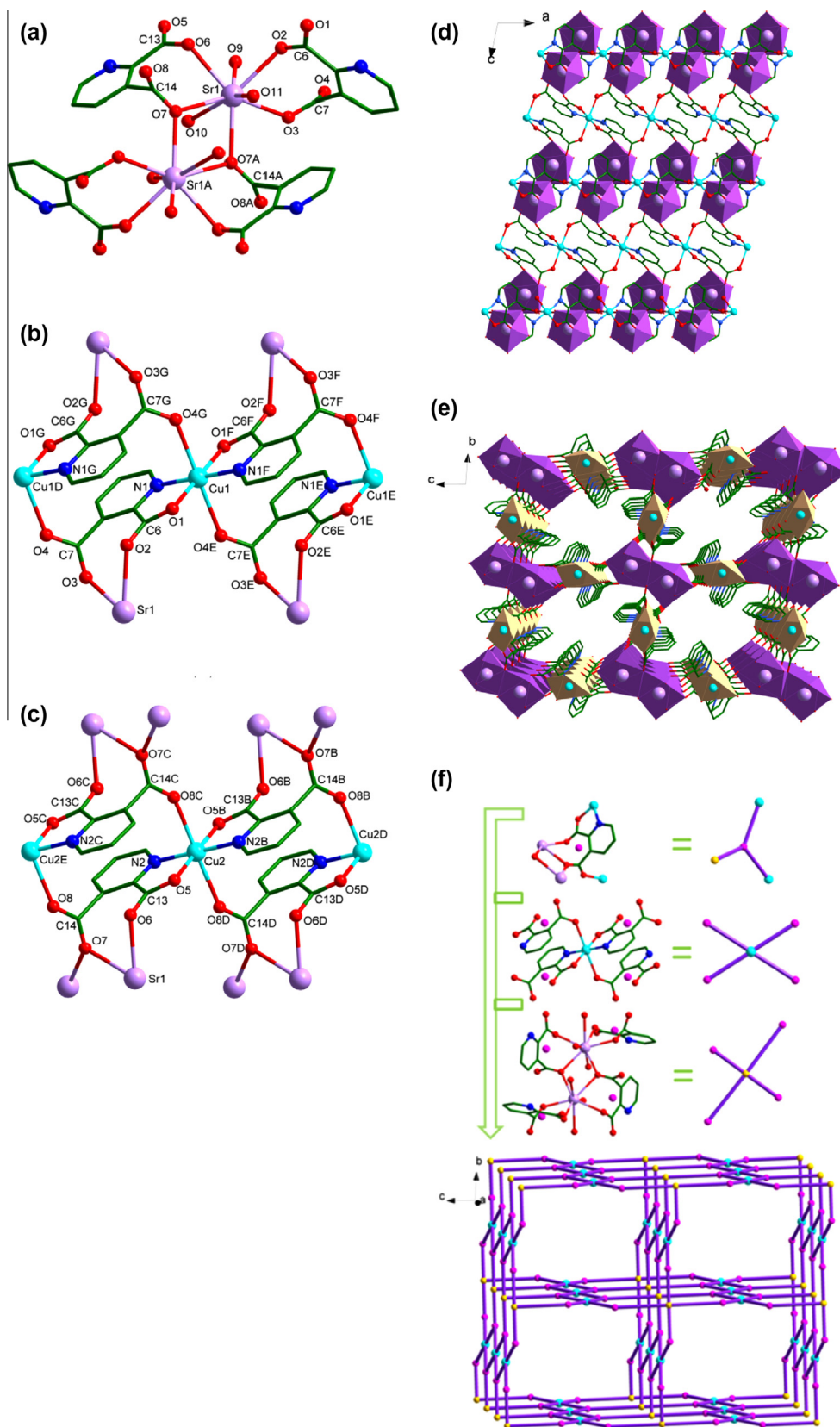


Fig. 3. (a) Coordination environments of the Sr1 ions in **5**. (b) Coordination environments of the Cu1 ions in **5**. (c) Coordination environments of the Cu2 ions in **5** (A: #1 $-x-1, -y+1, -z+2$; B: $-x, -y, -z+2$; C: $-x-1, -y, -z+2$; D: $x+1, y, z$; E: $x-1, y, z$; F: $-x-2, -y+1, -z+1$; G: $-x-1, -y+1, -z+1$). (d) The connection of Cu1 ions and $[\text{Sr}_2(\text{pydc})_4]^{4-}$ units in the *ac* plane. (e) The 3-D polyhedron framework structure of **5** viewed along the *a*-axis. (f) Schematic representation of the 5-nodal topology net with the topological notation $(4.8^2)_4(4^2.8^2.10^2)_2(8^6)$ in the *bc* plane. Hydrogen atoms and lattice water molecules are omitted for clarity. Color codes: lavender, Sr; turquoise, Cu; red, O; blue, N; green, C. (Colour online.)

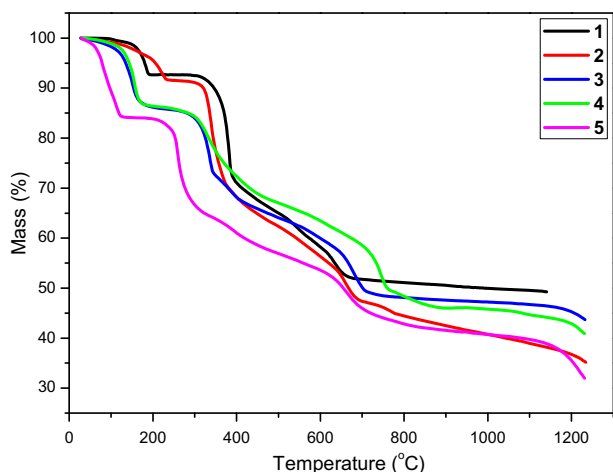


Fig. 4. The TGA curves of complexes 1–5.

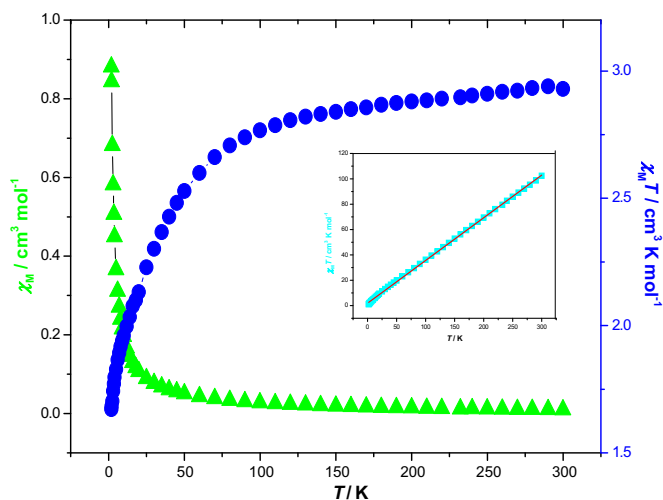


Fig. 5. Temperature dependence of the magnetic susceptibilities in the form of $\chi_M T$ vs. T and χ_M vs. T for **1** at 1 kOe. Inset: Temperature dependence of the magnetic susceptibilities in the form of $\chi_M^{-1} \nu T$ for **1** at 1 kOe. The solid line corresponds to the best fit from 300 to 2 K.

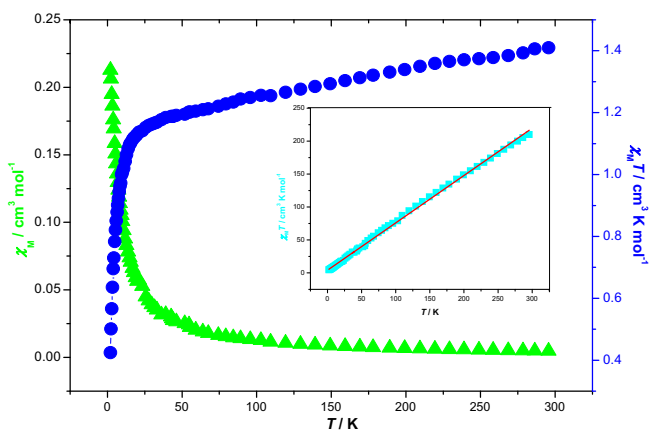


Fig. 6. Temperature dependence of the magnetic susceptibilities in the form of $\chi_M T$ vs. T and χ_M vs. T for **2** at 1 kOe. Inset: Temperature dependence of the magnetic susceptibilities in the form of $\chi_M^{-1} \nu T$ for **2** at 1 kOe. The solid line corresponds to the best fit from 300 to 2 K. (Colour online.)

$g = 2.0$, $S = 3/2$) for one Ni^{II} ion. As the temperature is lowered, the $\chi_M T$ value first decreases smoothly and then decreases abruptly to a minimum value of $0.42 \text{ cm}^3 \text{ K mol}^{-1}$ at 2 K. We endeavored to fit the experimental susceptibility using various models for the Ni(II) chain complex [48,49], but none of the results were well-pleasing. Fitting the data in the temperature range 2–300 K to the Curie–Weiss law gives a C value of $1.39 \text{ cm}^3 \text{ K mol}^{-1}$ and a θ value of -5.58 K . The negative value of θ indicates weak antiferromagnetic couplings between the Ni^{II} ions.

4. Conclusion

Five heteronuclear coordination polymers M^{II}–Sr^{II} (M = Co, Ni, Zn, Cu) based on pyridine 2,3-dicarboxylic acid (H₂pydc) have been synthesized for the first time. These complexes display three varieties of 3-D topological structures. The magnetic properties of complexes **1** and **2** have been determined and both of them show antiferromagnetic exchange interactions between the metal centers.

Acknowledgements

The authors appreciate the financial support from the Natural Science Foundation of China (21272167 and 21201127), A project funded by the Priority Academic Program Development of Jiangsu Higher Education Institution, Graduate Education Innovation Project in Jiangsu Province (CXZZ12_0808), Qinghai Science & Technology Department of China (2011-G-208 and 2011-Z-722), and KLSLRC (KLSLRC-KF-13-HX-1).

Appendix A. Supplementary data

CCDC 948529, 948485, 948484, 948483 and 948528 contain the supplementary crystallographic data for complexes **1–5**, respectively. These data can be obtained free of charge via <http://www.ccdc.cam.ac.uk/conts/retrieving.html>, or from the Cambridge Crystallographic Data Centre, 12 Union Road, Cambridge CB2 1EZ, UK; fax: (+44) 1223-336-033; or e-mail: deposit@ccdc.cam.ac.uk. For tables of selected bond lengths and angles, additional figures of these complexes and other electronic formats see supporting information. Supplementary data associated with this article can be found, in the online version, at <http://dx.doi.org/10.1016/j.poly.2013.12.042>.

References

- [1] R. Cao, J. Lü, S.R. Batten, *CrystEngComm* 10 (2008) 784.
- [2] K.M. Fromm, *Coord. Chem. Rev.* 252 (2008) 856.
- [3] S. Harder, *Angew. Chem., Int. Ed.* 42 (2003) 3430.
- [4] Y. Zhang, X.B. Luo, Z.L. Yang, G. Li, *CrystEngComm* 14 (2012) 7382.
- [5] X. Lin, D.M. Doble, A.J. Blake, A. Harrison, C. Wilson, M. Schroder, *J. Am. Chem. Soc.* 125 (2003) 9476.
- [6] Y.M. Chen, L.N. Zheng, S.X. She, Z. Chen, B. Hu, Y.H. Li, *Dalton Trans.* 40 (2011) 4970.
- [7] X. Zhang, Y.Y. Huang, J.K. Cheng, Y.G. Yao, J. Zhang, F. Wang, *CrystEngComm* 14 (2012) 4843.
- [8] X. Zhang, Y.Y. Huang, Q.P. Lin, J. Zhang, Y.G. Yao, *Dalton Trans.* 42 (2013) 2294.
- [9] Y. Xu, Y.X. Che, F.Y. Cheng, J.M. Zheng, *Eur. J. Inorg. Chem.* 34 (2011) 5299.
- [10] X.Q. Zhao, Y. Zuo, D.L. Gao, B. Zhao, W. Shi, P. Cheng, *Cryst. Growth Des.* 9 (2009) 3948.
- [11] A. Zurawski, J.C. Rybak, L.V. Meyer, P.R. Matthes, V. Stepanenko, N. Dannenbauer, F. Wurthner, K. Müller-Buschbaum, *Dalton Trans.* 41 (2012) 4067.
- [12] J.M. Hamilton, M.J. Anhorn, K.A. Oscarson, J.H. Reibenspies, R.D. Hancock, *Inorg. Chem.* 50 (2011) 2764.
- [13] B.D. Chandler, D.T. Cramb, G.K.H. Shimizu, *J. Am. Chem. Soc.* 128 (2006) 10403.
- [14] W.J. Evans, D.G. Giarikos, M.A. Greci, J.W. Ziller, *Eur. J. Inorg. Chem.* (2002) 453.
- [15] G.B. Deacon, C.M. Forsyth, P.C. Junk, A. Urbatsch, *Eur. J. Inorg. Chem.* (2010) 2787.
- [16] B.D. Chandler, A.P. Côté, D.T. Cramb, J.M. Hill, G.K.H. Shimizu, *Chem. Commun.* (2002) 1900.

- [17] G. Swarnabala, M.V. Rajasekharan, *Inorg. Chem.* 37 (1998) 1483.
- [18] A. Barge, M. Botta, U. Casellato, S. Tamburini, P.A. Vigato, *Eur. J. Inorg. Chem.* (2005) 1492.
- [19] M. Li, L. Yuan, H. Li, J. Sun, *Inorg. Chem. Commun.* 10 (2007) 1281.
- [20] Y.M. Chen, Y.Y. Cao, W.Q. Chen, Q. Gao, L. Li, D.D. Gao, W. Liu, Y.H. Li, W. Li, *Dalton Trans.* 42 (2013) 10011.
- [21] Y.M. Chen, W.Q. Chen, Z.H. Ju, Q. Gao, T. Lei, W. Liu, Y.H. Li, D.D. Gao, W. Li, *Dalton Trans.* 42 (2013) 10495.
- [22] A. Lazarescu, S. Shova, J. Bartolome, P. Alonso, A. Arauzo, A.M. Balu, Y.A. Simonov, M. Gdaniec, C. Turta, G. Filoti, R. Luque, *Dalton Trans.* 40 (2011) 463.
- [23] B. Barszcz, M. Hodorowicz, A. Jabłońska-Wawrzycka, J. Masternak, W. Nitek, K. Stadnicka, *Polyhedron* 29 (2010) 1191.
- [24] W. Starosta, J. Leciejewicz, *J. Coord. Chem.* 62 (2009) 1240.
- [25] P. Mahata, K.V. Ramya, S. Natarajan, *Chem. Eur. J.* 14 (2008) 5839.
- [26] M. Frisch, C.L. Cahill, *Cryst. Growth Des.* 8 (2008) 2921.
- [27] M. Li, J. Xiang, L. Yuan, S. Wu, S. Chen, J. Sun, *Cryst. Growth Des.* 6 (2006) 2036.
- [28] G.H. Wang, Z.G. Li, H.Q. Jia, N.H. Hu, J.W. Xu, *CrystEngComm* 11 (2009) 292.
- [29] H.T. Zhang, Y.Z. Li, H.Q. Wang, E.N. Ni, X.Z. You, *CrystEngComm* 7 (2005) 578.
- [30] S. Yan, X. Li, X. Zheng, *J. Mol. Struct.* 929 (2009) 105.
- [31] H. Yin, S.X. Liu, *J. Mol. Struct.* 918 (2009) 165.
- [32] T.K. Maji, G. Mostafa, R. Matsuda, S. Kitagawa, *J. Am. Chem. Soc.* 127 (2005) 17152.
- [33] B.O. Patrick, C.L. Stevens, A. Storr, R.C. Thompson, *Polyhedron* 22 (2003) 3025.
- [34] G.M. Sheldrick, *SHELXS 97 Program for the Solution of Crystal Structures*, University of Göttingen, Germany, 1997.
- [35] G.M. Sheldrick, *SHELXL 97, Program for the Refinement of Crystal Structures*, University of Göttingen, Germany, 1997.
- [36] G.M. Sheldrick, *Acta Crystallogr., Sect. A* 64 (2008) 112.
- [37] Y.M. Chen, S.X. She, L.N. Zheng, B. Hu, W.Q. Chen, B. Xu, Z. Chen, F.Y. Zhou, Y.H. Li, *Polyhedron* 30 (2011) 3010.
- [38] K. Tang, R. Yun, Z. Lu, L. Du, M. Zhang, Q. Wang, H. Liu, *Cryst. Growth Des.* 13 (2013) 1382.
- [39] M. O'Keeffe, O.M. Yaghi, *Chem. Rev.* 112 (2012) 675.
- [40] B.E. Applegate, T.A. Barckholtz, T.A. Miller, *Chem. Soc. Rev.* 32 (2003) 38.
- [41] M.A. Halcrow, *Chem. Soc. Rev.* 42 (2013) 1784.
- [42] A.K. Boudalis, C.P. Raptopoulou, B. Abarca, R. Ballesteros, M. Chadlaoui, J.P. Tuchagues, A. Terzis, *Angew. Chem., Int. Ed.* 45 (2006) 432.
- [43] X.N. Cheng, W.X. Zhang, Y.Z. Zheng, X.M. Chen, *Chem. Commun.* 34 (2006) 3603.
- [44] M. Kurmoo, H. Kumagai, S.M. Hughes, C.J. Kepert, *Inorg. Chem.* 42 (2003) 6709.
- [45] T. Yi, C. Ho-Chol, S. Gao, S. Kitagawa, *Eur. J. Inorg. Chem.* (2006) 1381.
- [46] X.X. Hu, J.Q. Xu, P. Cheng, X.Y. Chen, X.B. Cui, J.F. Song, G.D. Yang, T.G. Wang, *Inorg. Chem.* 43 (2004) 2261.
- [47] M.E. Fisher, *Am. J. Phys.* 32 (1964) 343.
- [48] J.J. Borrás-Almenar, E. Coronado, J. Curely, R. Georges, *Inorg. Chem.* 34 (1995) 2699.
- [49] F. Meyer, U. Ruschewitz, P. Schober, B. Antelmann, L. Zsolnai, *J. Chem. Soc., Dalton Trans.* (1998) 1181.